Microscopic theory for a ferromagnetic nanowire/superconductor heterostructure: Transport, fluctuations, and topological superconductivity

So Takei[1] and Victor Galitski[1,2,3]

[1]*Condensed Matter Theory Center, The Department of Physics, The University of Maryland, College Park, Maryland 20742-4111, USA*

[2]*Joint Quantum Institute, The University of Maryland, College Park, Maryland 20742-4111, USA*

[3]*Kavli Institute for Theoretical Physics, University of California at Santa Barbara, Santa Barbara, California 93106-4030, USA*

(Received 7 April 2012; published 28 August 2012)

Motivated by the recent experiment of Wang *et al*. [Nat. Phys. **6**, 389 (2010)], who observed a highly unusual transport behavior of ferromagnetic cobalt nanowires proximity-coupled to superconducting electrodes, we study the proximity effect and temperature-dependent transport in such a mesoscopic hybrid structure. It is assumed that the asymmetry in the tunneling barrier gives rise to the Rashba spin-orbit coupling in the barrier that enables induced p-wave superconductivity in the ferromagnet to exist. We first develop a microscopic theory of Andreev scattering at the spin-orbit-coupled interface, derive a set of self-consistent boundary conditions, and find an expression for the p-wave minigap in terms of the microscopic parameters of the contact. Second, we study the temperature dependence of the resistance near the superconducting transition, and we find that it should generally feature a fluctuation-induced peak. The upturn in resistance is related to the suppression of the single-particle density of states due to the formation of fluctuating pairs, whose tunneling is suppressed. In conclusion, we discuss this and related setups involving ferromagnetic nanowires in the context of one-dimensional topological superconductors. It is argued that to realize unpaired end Majorana modes, one does not necessarily need a half-metallic state; a partial spin polarization may suffice. Finally, we propose yet another related class of material systems—ferromagnetic semiconductor wires coupled to ferromagnetic superconductors—where direct realization of the Kitaev-Majorana model should be especially straightforward.

DOI: 10.1103/PhysRevB.86.054521 PACS number(s): 74.40.−n, 74.45.+c, 73.40.−c

I. INTRODUCTION

The coexistence of ferromagnetism and superconductivity is a rare phenomenon, yet there exists unambiguous evidence for its occurrence. Superconductivity has been thoroughly investigated in uranium-based itinerant ferromagnets,[1–4] and there have been reports on the possible coexistence of these phases in the d-electron compound $ZrZn_2$ (Ref. 5) and the copper oxide compound $RuSr_2GdCu_2O_{8-\delta}$ (Ru-1212).[6–9] Neutron diffraction measurements in ferromagnetic superconductors $ErRh_4B_4$,[10] $HoMo_6S_8$,[11] and $HoMo_6Se_8$ (Ref. 12) indicate an inhomogeneous magnetic order coexisting with superconductivity. More recently, the coexistence of these seemingly exclusive states was also seen in Pb/PbO core/shell nanoparticles[13] and in two-dimensional interfaces between perovskite band insulators $LaAlO_3$ and $SrTiO_3$.[14,15]

The interplay of superconductivity and ferromagnetism can also be studied in the context of the superconducting proximity effect, where a superconductor in contact with a normal metal induces superconducting correlations in the latter. Due to incompatible spin ordering, conventional superconducting correlations typically penetrate negligibly inside a ferromagnet.[16] However, a number of recent experimental studies have demonstrated an unexpectedly long-ranged proximity effect in mesoscopic superconductor-ferromagnet hybrid structures.[17–22] There are a number of theoretical scenarios which can explain this phenomenon. In most of the scenarios, pair correlations inside the ferromagnet are attributed to some type of equal-spin triplet pairing. In one case, the long-ranged proximity effect is attributed to spin-triplet odd-frequency s-wave pairing which can be induced when magnetization inhomogeneity is present near the interface.[23,24] This beautiful theory, which predicts an exotic odd-frequency (even-momentum) symmetry for the triplet component of the condensate, was originally suggested by Berenzinskii as a possible phase in superfluid ^{3}He.[25] Other theoretical works have investigated Josephson coupling between two conventional superconductors separated by a half-metallic ferromagnet, and singlet-triplet conversion due to a spin-active interface was studied.[26,27] In a clean and purely one-dimensional (1D) junction, it was recently shown that singlet pairing can also account for the long-ranged proximity effect in a ferromagnet.[28,29]

Seemingly unrelated to the developments in the superconducting proximity effect at the time, Kitaev showed in his pioneering work that Majorana fermion excitations can be localized at the ends of a spinless $p_x + ip_y$ superconducting quantum wire.[30] Conceptually, the Kitaev model of a topological superconductor is that of a fully polarized ferromagnetic superconductor. However, a direct connection between the model and the existing hybrid superconducting systems has been made only recently. In some of the recent proposals, the superconducting proximity effect plays a key role in realizing topological superconductors which support Majorana fermions on their boundaries or in vortex cores.[31–45]

On the experimental front, Ref. 21 has shown that a ferromagnetic cobalt (Co) quantum wire can be made superconducting by placing it in contact with a conventional superconductor. Proximity-induced superconductivity was observed in the wire over a distance of a few hundred nanometers. While the exact nature of the pairing symmetry still remains open, if the proximity effect can be attributed to triplet p-wave pairing, the experiment of the kind in Ref. 21 is very close to realizing

 ©2012 American Physical Society

a topological superconductor,[30] and can host the sought-after Majorana fermions at the two ends of the wire.

With its broader physical relevance aside, the experimental work of Ref. 21 included interesting observations in the context of the superconducting proximity effect in ferromagnetic systems. The work systematically studies the resistance of ferromagnetic single-crystal cobalt nanowires sandwiched between two superconducting electrodes made out of tungsten (W). Proximity-induced superconductivity is observed in the nanowire over a distance of order 500 nm, which is orders of magnitude longer than the coherence length expected for conventional superconducting correlations inside a ferromagnet. For some wires, the transition to superconductivity is preceded by a large and sharp resistance peak near the transition temperature of the electrodes. The resistance peak disappears when the Co wire is replaced by a gold wire, suggesting an intimate connection between it and the ferromagnetism of the wire. We note that similar resistance peaks have been observed in various superconducting hybrid structures in the past.[46–51] However, the authors of Ref. 21 claim that the peaks observed in their experiment are distinct from those attributed to nonequilibrium charge imbalance[46–49] and spin accumulation[50,51] effects. This invites a search for an alternative mechanism behind the resistance peak.

Motivated by these observations, we study temperature-dependent transport through a ferromagnetic Co nanowire coupled to conventional superconductor W electrodes. The main goal is to provide a perspective on the origin of the resistance peak based on the physics of superconducting fluctuations[52,53] in the W electrodes. We discuss a possible faithful model for the Co nanowire in the vicinity of the deposited W electrodes, develop a microscopic theory for the superconducting fluctuations in the W electrodes, and study how these fluctuations influence the transport through the Co wire. We focus on the resistance across a W-Co interface, which we argue is the dominant source of impedance in the transport. Our superconducting fluctuations theory for the resistance peak depends crucially on the proximity effect scenario for the long-ranged proximity effect in the Co nanowire. In this work, we consider a scenario in which the asymmetry at the W-Co interface gives rise to the Rashba spin-orbit coupling there[54,55] and enables equal-spin triplet p-wave superconductivity to be induced inside the ferromagnet.

We emphasize that the Co wire throughout the work is treated in the ballistic/ballistic-to-diffusive crossover limit. As we show in later sections of the paper, the treatment of the wire in this limit is reasonably justified based on experimental data[21] and past studies on Co band structure.[56–59] The information available to us is insufficient to determine the nature of proximity-induced superconductivity in the nanowire. As we have mentioned above, the odd-frequency s-wave proximity effect,[23,24] studied in the context of diffusive ferromagnets, remains a realistic scenario here. It is well known that the conversion from singlet to triplet superconductivity within this scenario occurs due to some form of inhomogeneous magnetic moments near the interface. However, the cobalt wire studied in Ref. 21 is single domain, so such inhomogeneities may not be the mechanism behind the singlet-triplet conversion. In a 1D junction, the long-ranged proximity effect of singlet pairs is possible in a clean ferromagnet due to the absence of destructive interference among various transverse channels, which usually leads to the short-ranged proximity effect in higher dimensions.[28,29] Indeed, in Ref. 28 the long-ranged proximity effect observed in Ref. 21 was attributed to singlet pairs. However, the Co wires are 40–80 nm wide, and hence it is not clear if they can be considered in the purely 1D limit. Here, we explore the possibility of an *even-frequency* p-wave proximity effect induced via interfacial spin-orbit coupling, which is another viable physical scenario when the ferromagnet is in the clean limit. As we argue below, this p-wave proximity effect may survive even in disordered systems due to mesoscopic fluctuation effects. Also, it was recently noted that surface states of certain heavy metals can host strong Rashba spin-orbit coupling.[60] For the Au(111) surface, Rashba splitting of order 50 meV has been observed,[61] while for the Ag(111) surface alloyed with Bi and Pb, this can be as large as 0.5 eV.[62] Since W is also a heavy atom, it is not unreasonable to assume that the surface of the tungsten electrodes can also host a relatively large spin-orbit coupling.

The paper is organized as follows. Section II summarizes the main findings of the experiment in Ref. 21, with a particular focus on the anomalous resistance peak. The section also provides an estimate for the mean-free path of the Co wire and a justification for considering it in the clean limit. In Sec. III, we provide a heuristic picture for how the superconducting fluctuations can explain the resistance peak. The heuristic picture is then substantiated by microscopic calculations in Secs. IV and V. A summary and conclusions are presented in Sec. VI, where a possible connection between the experiment and topological superconductivity is also outlined.

II. SUMMARY OF THE EXPERIMENT

Reference 21 reports observations of the long-ranged proximity effect in single-crystal ferromagnetic Co nanowires. Resistance of the wire is studied using a four-probe setup with all four electrodes made from superconducting W [see Fig. 1(a)] or with a combination of superconducting W and nonsuperconducting platinum (Pt) electrodes [see Fig. 1(b)]. While the outer electrodes are used to pass current i_w through the wire, the inner electrodes are used to measure the potential difference V across a length L of the wire. The experiment focuses on the resistance of the Co wire defined via $R = V/i_w$. With W voltage electrodes [as in Fig. 1(a)], Co wires show evidence of superconductivity below the transition temperature of the electrodes even for $L \sim 1$ μm. Such a resistance drop is not observed when the superconducting electrodes are replaced by Pt. However, when an additional electrically isolated W strip is deposited between the Pt electrodes [see Fig. 1(c)], proximity-induced superconducting properties are restored in the Co wire.

A. The resistance peak

The experiment observes a sharp peak in the resistance R as a function of temperature as it approaches the superconducting transition temperature of the W electrodes. An illustration of the observed resistance versus temperature is shown in Fig. 2.

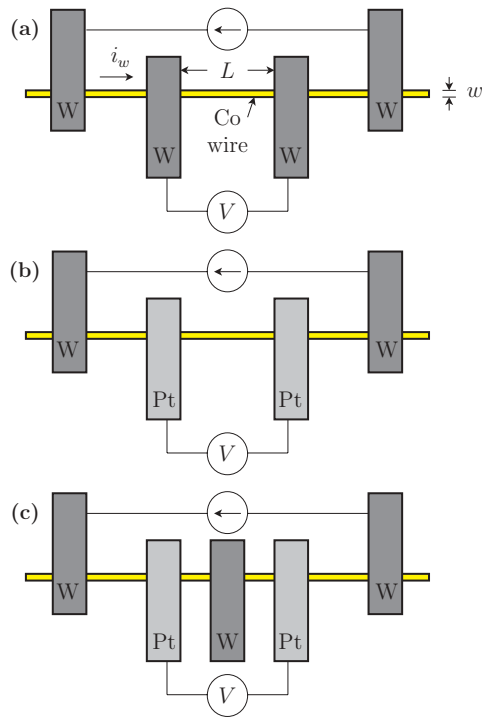

FIG. 1. (Color online) A cartoon representation of the various experimental setups used in Ref. 21. Three main setups are considered: (a) W current and voltage electrodes; (b) W current electrodes and Pt voltage electrodes; and (c) same as (b) with an additional electrically isolated W strip between the Pt electrodes. Length of the wire L is determined by the distance between the inner edges of the voltage electrodes. The width (or diameter) of the Co wire is denoted by w.

The transition temperature of the electrodes is estimated to be between $T_c = 4.4$ and 5 K. This resistance peak is very large and constitutes 25–100% of the normal state resistance depending on the wire width. Intriguingly, the peak disappears when the Co wire is replaced by a nonferromagnetic gold wire, and thus seems to be a consequence of the ferromagnetism of the Co wire. The large resistance peak (along with the proximity effect) also disappears when the W electrodes are replaced by Pt electrodes [see Fig. 1(b)], but is restored once an additional electrically isolated W strip is deposited [see Fig. 1(c)]. The large resistance upturn thus seems to require only that a superconducting strip is in contact with the nanowire, and does not require it to be either a current or a voltage electrode.

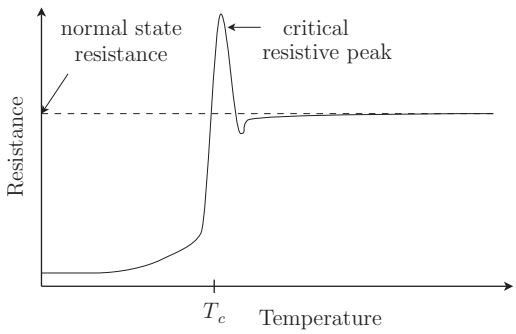

FIG. 2. An illustration of the experimentally observed Co wire resistance as a function of temperature. A critical resistance peak is observed near the transition temperature T_c of the W electrodes. A precipitous drop in the resistance is then observed below T_c.

B. Mean-free path of the Co nanowire

When the extra W strip is deposited on the wire [see Fig. 1(c)], data show that the wire's normal state resistance increases by approximately 55 Ω. This amounts to a nearly 50% increase from its normal state resistance of ≈126 Ω prior to the deposition [setup as shown in Fig. 1(b)]. This suggests that the deposition process could have strongly modified the property of the wire in the vicinity of the contact. Returning to the setup in Fig. 1(a), the experimental data show a total normal state wire resistance of approximately 145 Ω. The resistance of the Co wire arising from regions unaffected by the W strips may then be approximated as $145\ \Omega - 2 \times 55\ \Omega = 35\ \Omega$. Using the quoted distance between the voltage electrodes (i.e., $L = 1.5\ \mu$m) and the wire width (i.e., $w = 36$ nm), the corresponding resistivity is $\rho \approx 23\ \text{n}\Omega\,\text{m}$. An estimate for Co's Fermi velocity, based on critical current oscillations observed in a Nb/Co/Nb Josephson junction, gives $v_F \approx 280$ km/s.[63] From this, the density for electrons with a single spin projection can be estimated as

$$n = x^3 \frac{m_e^3 v_F^3}{6\pi^2 \hbar^3} \approx x^3 2.4 \times 10^{26}\ \text{m}^{-3}, \tag{1}$$

where $x = m^*/m_e$ is the Co effective mass ratio, with m^* being the effective mass of the Co electrons and m_e the mass of the electron. The Drude formula then gives a mean-free path estimate of

$$\ell = \frac{x m_e v_F}{n e^2 \rho} \approx \frac{1.8\ \mu\text{m}}{x^2}. \tag{2}$$

Cores of the Co nanowires studied in Ref. 21 show a hexagonal close-packed zone pattern, and the wires have a [0001] growth direction. Presumably, the electron transport through the wire is then along the c-axis direction. For our estimate of the Co effective mass x, we use results based on band-structure calculations for Co cyclotron mass.[59] In the relevant direction of transport, we have $x \approx 3$. Inserting this value into (2), the mean-free path is estimated to be $\ell \approx 200$ nm, which is the same order of magnitude as the observed coherence length in the Co wire. Within this scenario, the region of the Co wire unaffected by the W electrodes is in the ballistic-to-diffusive crossover regime.

We note, however, that the above estimate for the mean-free path relies crucially on our estimate for the resistance of the Co wire unaffected by the W electrodes. Furthermore, the estimate also depends sensitively on the values used for v_F and x, which we do not know with complete certainty. Due to Co's complicated band structure, the values for v_F and x depend strongly on the direction of transport with respect to the crystallographic axes and on the Fermi surface which gives the dominant contribution to transport. For instance, for $v_F \sim 10^6$ m/s (quoted in Ref. 21), we obtain a much shorter mean-free path of $\ell \approx 16$ nm, implying that the wire is in the diffusive limit. Co having multiple subbands with varying x also implies that some subbands are less affected by disorder than others. If all bands participating in transport indeed have short mean-free paths (of the order of a few

nanometers), the likely mechanism for the proximity effect is the spatially even, odd-frequency pairing.[23,24] However, based on experimental data in Ref. 21 and on the Co band structure and de Haas–van Alphen studies relevant for electron transport in the c-axis direction,[59] we have shown above that there is reasonable justification to model the Co wire in the clean limit, and the even-frequency p-wave pairing is a viable mechanism for the observed proximity effect. Furthermore, mesoscopic fluctuation effects may further enable remnants of p-wave superconductivity to persist well into the diffusive limit.[64] In this work, we pursue this scenario of a Co wire with proximity-induced p-wave superconductivity, and we purport that it provides an explanation for the resistance peak.

III. RESISTANCE PEAK DUE TO SUPERCONDUCTING FLUCTUATIONS—A HEURISTIC PICTURE

We begin by providing a heuristic picture for how superconducting fluctuations, which exist inside the W electrodes above their critical temperature, can give rise to the observed resistance peak. While similar resistance peaks in superconducting hybrid structures have been attributed to, for instance, nonequilibrium charge imbalance[46–49] and spin accumulation[50,51] effects, Ref. 21 has ruled these scenarios out for their observations. Therefore, the goal of this section is to provide a superconducting fluctuations perspective on the peak which is distinct from other mechanisms considered thus far in this context. Based on the experimental observations and data, we adopt a physical picture in which most of the resistance comes from interfaces between Co and W. Within our picture, the combination of superconducting fluctuations and suppressed transport across W-Co interfaces work together to give a natural explanation for the peak.

We argued in Sec. II B that the W electrodes have a strong impact on the transport properties through the Co wire. We reiterate the experimental fact that when the extra W strip is deposited on top of the Co wire [see Fig. 1(c)], the normal state resistance of the wire increases by nearly 50%. This indicates that when a W electrode is deposited onto the nanowire, it modifies the wire in its vicinity and provide a major source of resistance. A faithful model of the Co wire may then be such that the majority of the current i_w goes through the two W voltage electrodes. If this view is adopted, this creates multiple W-Co interfaces, and the electron transport through the Co wire is expected to be strongly modified by Andreev physics at the W-Co interfaces. The Andreev physics at the W-Co interface in the presence of Rashba spin-orbit-coupled barrier will be discussed in Sec. IV.

The observed resistance peak is very reminiscent of similar anomalous peaks studied in the context of c-axis transport in cuprate superconductors,[65–67] magnetoresistance in dirty films,[68] as well as magnetoresistance in granular electronic systems.[69] In all these cases, the anomalous peak has been explained using the phenomenon of superconducting fluctuations.[52,53] This phenomenon is associated with fluctuating Cooper pairs that form while the system is in the normal state but just above the transition temperature T_c. The appearance of Cooper pairs above T_c opens up a new channel for charge transport. Indeed, these fluctuating Cooper pairs can be treated as carriers of charge $2e$ with a lifetime given by $\tau_{\rm GL} \sim \hbar/k_B(T - T_c)$. This leads to a contribution to the conductivity known as the Aslamazov-Larkin (AL) contribution or paraconductivity, and it gives a positive correction to the Drude conductivity. There is also an indirect correction known as the density of states (DOS) contribution. One of the important consequences of these fluctuating Cooper pairs is the decrease in the single-particle DOS near the Fermi level. The idea is that if some electrons are involved in pairing, they cannot simultaneously participate in single-electron transport. The DOS contribution, therefore, gives a negative correction to the Drude conductivity.

As we approach T_c of the W electrodes from above, Cooper pair fluctuations grow inside the W electrodes. By virtue of the interface Rashba spin-orbit coupling at the W-Co interfaces, singlet Cooper pairs inside W can be converted and triplet pairs can permeate into the Co wire. Pair transport correction to the conductivity arises due to the transport of these fluctuating Cooper pairs through the interface. However, pair tunneling across an interface is strongly suppressed because it is a higher-order process in both tunneling and the singlet-triplet conversion rate, which requires a spin flip process enabled only by weak interfacial spin-orbit coupling. On the other hand, the DOS contribution to conductivity is associated with single-particle transport and is thus lower order in tunneling and requires no spin flip. We therefore qualitatively expect the DOS correction to be parametrically larger than the pair transport contribution, thus giving a negative overall correction to the Drude conductivity. This clearly can explain the anomalous upturn in the resistance as a function of temperature. We note that the *tunneling nature* of transport across the interface is extremely important for the DOS correction to dominate over the pair transport contribution. In the usual theory of superconducting fluctuations for the bulk of a superconductor, the pair transport contribution (Aslamazov-Larkin contribution) is typically dominant over the DOS contribution and the resistance upturn is not observed.[52]

When the Co wire is replaced by a gold wire, the situation is modified. Since gold is not ferromagnetic, singlet correlations are expected to survive over a much longer distance inside the wire. In this case, Cooper pair tunneling across the W-Au interface is much more transparent since it does not require a spin flip. Therefore, Cooper pairs are more efficient at transporting charge, and the pair transport contribution is expected to dominate over the DOS contribution. Here, we purport that the absence of the resistance peak in the Au wire can be explained if indeed the pair transport contribution to the conductivity is parametrically larger than the DOS contribution, thus giving an overall positive correction to conductivity.

Near the superconducting transition temperature and in dimensions at or below 2, both AL (Ref. 70) and DOS contributions show either algebraic or logarithmic divergent behavior as a function of $(T - T_c)$. Denoting the divergent part of the AL corrections by the function $f_{\rm AL}(T - T_c)$ and the divergent part of the DOS correction by $f_{\rm DOS}(T - T_c)$ (and ignoring the Maki-Thompson contribution), the total superconducting fluctuation correction to the normal resistance R_0 can be schematically written as

$$\frac{\delta R(T)}{R_0} = A_{\rm DOS} f_{\rm DOS}(T - T_c) - A_{\rm AL} f_{\rm AL}(T - T_c), \quad (3)$$

where $A_{\rm AL}$ and $A_{\rm DOS}$ are positive prefactors. As we will show in Sec. V, $f_{\rm AL} \propto (T/T_c - 1)^{-4}$, while $f_{\rm DOS} \propto (T/T_c - 1)^{-1/2}$, indicating that the AL contribution diverges much more strongly than the DOS term as $T \to T_c^+$. Therefore, unless the prefactor $A_{\rm AL}$ is very small in comparison to $A_{\rm DOS}$, the DOS contribution is always parametrically smaller than the AL contribution and the conductivity correction is positive. This leads to a monotonic decrease in the resistance as the system approaches the transition, and no peak will result. However, if we have a situation in which the AL prefactor is greatly suppressed, i.e., $A_{\rm AL} \ll A_{\rm DOS}$, the DOS contributions may be sufficiently larger than the AL counterpart for T, but not too close to T_c^+. In this case, the resistivity can display an upturn before the AL contribution eventually takes over and the resistivity makes a precipitous fall as $T \to T_c^+$. We will argue below that the weak interfacial spin-orbit coupling can indeed provide a situation in which $A_{\rm AL} \ll A_{\rm DOS}$.

In the following sections, we will substantiate this heuristic picture with more microscopic calculations. We first consider the Andreev physics at a Rashba spin-orbited coupled interface between a ferromagnet and a conventional superconductor. We then provide a microscopic calculation which shows how the suppression of the density of states in the W electrodes leads to an increase in the resistance across the W-Co interface. We then provide a phenomenological calculation to show the resistance correction arising from Cooper pair transport across the interface.

IV. ANDREEV REFLECTION AT A FM-SC INTERFACE WITH RASHBA SPIN-ORBIT COUPLING

In this section, we focus on the Andreev physics which takes place at a W-Co interface, and we provide a microscopic expression for the induced minigap in the ferromagnet just near the interface. In the presence of interface Rashba spin-orbit coupling, we show that the induced triplet minigap has p-wave orbital character and that its magnitude is strongly suppressed by the weak spin-orbit coupling. The results of this section imply that spin-orbit-assisted pair transport across the W-Co interface is suppressed by the weakness of the spin-orbit coupling. These results will play an important role in Sec. V, where we will develop a theory for the resistance peak.

The scenario we consider is a conventional superconductor (W) in contact with a (clean) itinerant ferromagnet (Co) which are separated by a low-transparency barrier with Rashba spin-orbit coupling.[54,55] The tunnel junction consists of a ferromagnetic metal at $0 \leqslant z < d$, a tunneling barrier at $-a < z < 0$, and a superconductor at $z \leqslant -a$ (see Fig. 3). For simplicity, we consider a planar junction where we retain translational symmetry in the direction(s) parallel to the interfaces. While this is not true to the geometry considered in Ref. 21, the main result of this section still applies to the experiment of interest. The derivation below closely follows Refs. 71 and 72, but is generalized to include spin-orbit-coupling effects in the barrier.

A. Equations of motion

The electron field operators in the ferromagnet $\psi^{(F)}$, tunnel barrier $\psi^{(B)}$, and superconductor $\psi^{(S)}$ satisfy the following

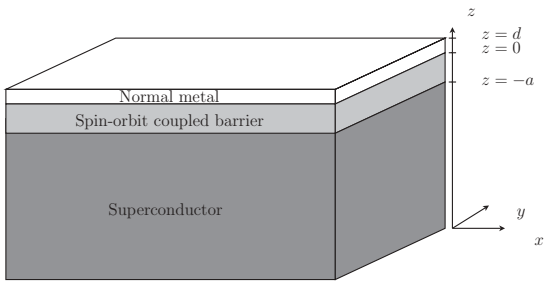

FIG. 3. The considered proximity tunnel junction. The ferromagnetic normal metal, the tunnel barrier with spin-orbit coupling, and the superconductor occupy $0 \leqslant z \leqslant d$, $-a < z < 0$, and $z \leqslant -a$, respectively.

equations of motion. In the normal region ($0 \leqslant z < d$),

$$\left[\left(\varepsilon - \xi_{\mathbf{p}}^{(F)} + \frac{\hbar^2\partial_z^2}{2m_F}\right)\delta_{\alpha\beta} - (\boldsymbol{h}\cdot\boldsymbol{\sigma}_{\alpha\beta})\right]\psi_{\beta,\mathbf{p}}^{(F)}(z) = 0; \quad (4)$$

in the barrier ($-a < z < 0$),

$$\left[\left(\varepsilon - U_0 - \frac{\mathbf{p}^2 - \hbar^2\partial_z^2}{2m_B}\right)\delta_{\alpha\beta} - \alpha_R[\boldsymbol{p}\times\boldsymbol{\sigma}_{\alpha\beta}]_z\right]\psi_{\beta,\mathbf{p}}^{(B)}(z) = 0; \quad (5)$$

and in the superconductor ($z \leqslant -a$),

$$\left(\varepsilon - \xi_{\mathbf{p}}^{(S)} + \frac{\hbar^2\partial_z^2}{2m_S}\right)\psi_{\alpha,\mathbf{p}}^{(S)}(z) - \Delta_{\alpha\beta}\psi_{\beta,-\mathbf{p}}^{(S)\dagger}(z) = 0. \quad (6)$$

Here, $\mathbf{p} = (p_x, p_y)$ is the two-dimensional momentum parallel to the interface; $\hat{\boldsymbol{\sigma}} = (\hat{\sigma}_x, \hat{\sigma}_y, \hat{\sigma}_z)$ is the vector of Pauli matrices acting in spin space; $\xi_{\mathbf{p}}^{(F)} = \mathbf{p}^2/2m_F - \mu_F$ and $\xi_{\mathbf{p}}^{(S)} = \mathbf{p}^2/2m_S - \mu_S$ are the electronic spectra in the ferromagnet and superconductor; m_F, m_S, and m_B are the effective masses in the corresponding region; and μ_F and μ_S are the Fermi levels in the ferromagnet and superconductor. α and β here label the spin projections. We assume that the ferromagnet and superconductor are separated by a tunnel barrier of height U_0 that, due to mirror asymmetry with respect to reflections relative to the $z = -a/2$ plane, contains Rashba spin-orbit coupling characterized by parameter α_R. The ferromagnet is modeled as a Fermi gas in a Zeeman field $\boldsymbol{h}$. Finally, the superconductor is assumed to be of s-wave type and, consequently, the mean-field order parameter is momentum-independent and reads $\Delta_{\alpha\beta} = \Delta(i\sigma_{y,\alpha\beta})$.

As shown in Eq. (4), we are modeling the ferromagnetic region within the usual single-band Stoner model where a rigid gap in the two spin bands is introduced. While this is clearly an oversimplified model for Co, we note that the applicability of our superconductor fluctuations theory for the resistance peak should not rely crucially upon the microscopic details of the ferromagnetic region. The result, however, relies on the assumption that singlet correlations are strongly suppressed in the ferromagnet and that the observed superconducting correlations in the nanowire are mainly due to triplet pairing. It is this *requirement* to convert singlet pairs into triplet pairs at the W-Co interface that is an important ingredient within our theory. In our case, this conversion is provided by the interfacial Rashba spin-orbit coupling. Since this effect is expected to be small, the Cooper pair transport across the

W-Co interface is suppressed and consequently leads to the anomalous resistance peak. The heuristic picture has been provided in Sec. III, and more details will be presented in Sec. V. We also note here that itinerant ferromagnetism can also be established through spin bandwidth asymmetry[73] rather than the conventional Stoner picture. The consequences of this have been addressed in the context of the superconductor-ferromagnet proximity effect.[74]

Although the barrier is spin-orbit coupled, this coupling will not lead to any spin Hall effects at the boundaries $z = 0$ and $z = -a$. Consequently, there is no accumulation of spin and the basic ballistic boundary conditions are identical to those in the theory of a conventional tunnel junction, namely

$$\overrightarrow{\Psi}^{(F)}_{\mathbf{p}}(d) = 0, \tag{7}$$

$$\overrightarrow{\Psi}^{(F)}_{\mathbf{p}}(0) = \overrightarrow{\Psi}^{(B)}_{\mathbf{p}}(0), \qquad \overrightarrow{\Psi}^{(B)}_{\mathbf{p}}(-a) = \overrightarrow{\Psi}^{(S)}_{\mathbf{p}}(-a), \tag{8}$$

$$\frac{1}{m_F}\partial_z \overrightarrow{\Psi}^{(F)}_{\mathbf{p}}(0) = \frac{1}{m_B}\partial_z \overrightarrow{\Psi}^{(B)}_{\mathbf{p}}(0), \tag{9}$$

and

$$\frac{1}{m_B}\partial_z \overrightarrow{\Psi}^{(B)}_{\mathbf{p}}(-a) = \frac{1}{m_S}\partial_z \overrightarrow{\Psi}^{(S)}_{\mathbf{p}}(-a). \tag{10}$$

Here, we have introduced a four-component state vector in the combined spin-Nambu space,

$$\overrightarrow{\Psi}^{(\rho)}_{\mathbf{p}}(z) = \left(\psi^{(\rho)}_{\uparrow,\mathbf{p}}(z), \psi^{(\rho)}_{\downarrow,\mathbf{p}}(z), \psi^{(\rho)\dagger}_{\uparrow,-\mathbf{p}}(z), \psi^{(\rho)\dagger}_{\downarrow,-\mathbf{p}}(z)\right)^T, \tag{11}$$

where $\rho = S, B, F$ labels the different regions. The full set of equations (4)–(6) is formulated for electron field operators acting in Fock space. However, since these equations and boundary conditions (7)–(10) are all linear, the operator nature of the unknown functions is not germane and we may simply approach the problem as in single-particle quantum mechanics. The problem is then conceptually very simple and reduces to solving second-order differential equations, albeit with nontrivial boundary conditions.

B. Deriving closed boundary conditions for the ferromagnet

1. Tunnel barrier

Let us look for a solution in the tunnel barrier in the form $\psi^{(B)}_{\alpha,\mathbf{p}}(z) = Z(z)\mathcal{P}_\alpha(\mathbf{p})$, where the transverse wave function $Z(z)$ satisfies

$$-\frac{\hbar^2}{2m_B}Z'' + [U_0 - \varepsilon + \varepsilon^R(\mathbf{p})]Z = 0, \tag{12}$$

and the planar wave function $\mathcal{P}_\alpha(\mathbf{p})$ is a standard wave function of the Rashba problem,

$$\mathcal{P}^{\pm}(\mathbf{p}) = \frac{1}{\sqrt{2}}\begin{pmatrix} \pm 1 \\ -ie^{i\gamma_{\mathbf{p}}} \end{pmatrix}, \tag{13}$$

describing the helicity eigenstates with eigenvalues, $\varepsilon^R_\pm(\mathbf{p}) = \frac{\mathbf{p}^2}{2m_B} \pm \alpha_R|\mathbf{p}|$. The angle $\gamma_{\mathbf{p}}$ is defined via $\mathbf{p} = p(\cos\gamma_{\mathbf{p}}, \sin\gamma_{\mathbf{p}})$. The general solution in the barrier then reads

$$\psi^{(B)}_{\alpha,\mathbf{p}}(z) = [C_{++}e^{q_+ z} + C_{+-}e^{-q_+ z}]\mathcal{P}^+_\alpha(\mathbf{p}) + [C_{-+}e^{q_- z} + C_{--}e^{-q_- z}]\mathcal{P}^-_\alpha(\mathbf{p}), \tag{14}$$

where $q_\pm = \sqrt{\frac{2m_B}{\hbar^2}[U_0 - \varepsilon + \varepsilon^R_\pm(\mathbf{p})]}$. To guarantee real $q_\pm$, we assume that the spin-orbit interaction scale is smaller than the barrier height.

We now use (8) to determine the relations between the coefficients in Eq. (14) and the values of the wave function on the superconductor and ferromagnet boundaries. We find

$$C_{ll'} = \frac{l'}{4\sinh(q_l a)}(\mathcal{F}^l e^{l' q_l a} - \mathcal{S}^l), \tag{15}$$

where $l, l' = \pm$ and

$$\mathcal{F}^\pm = i\psi^{(F)}_{\downarrow,\mathbf{p}}(0)e^{-i\gamma_{\mathbf{p}}} \pm \psi^{(F)}_{\uparrow,\mathbf{p}}(0), \tag{16}$$

$$\mathcal{S}^\pm = i\psi^{(S)}_{\downarrow,\mathbf{p}}(-a)e^{-i\gamma_{\mathbf{p}}} \pm \psi^{(S)}_{\uparrow,\mathbf{p}}(-a). \tag{17}$$

2. Superconductor

We now match the tunnel-barrier solution (14) with the superconducting solution at the barrier-superconductor interface using boundary condition (10). We then find

$$\frac{m_B}{m_S}\psi^{(S)}_{\alpha,\mathbf{p}}(-a) = T_{\mathbf{p},\alpha\beta}\psi^{(F)}_{\beta,\mathbf{p}}(0) - R_{\mathbf{p},\alpha\beta}\psi^{(S)}_{\beta,\mathbf{p}}(-a). \tag{18}$$

The matrices in Eq. (18), which play an important role in the analysis of the Andreev scattering problem, are given by

$$\hat{T}_{\mathbf{p}} = \begin{pmatrix} \kappa_t & i\delta\kappa_t e^{-i\gamma_{\mathbf{p}}} \\ -i\delta\kappa_t e^{i\gamma_{\mathbf{p}}} & \kappa_t \end{pmatrix}, \tag{19}$$

$$\hat{R}_{\mathbf{p}} = \begin{pmatrix} \kappa & i\delta\kappa e^{-i\gamma_{\mathbf{p}}} \\ -i\delta\kappa e^{i\gamma_{\mathbf{p}}} & \kappa \end{pmatrix}. \tag{20}$$

Here, we have defined

$$\kappa_t = \frac{q_+}{2\sinh(q_+ a)} + \frac{q_-}{2\sinh(q_- a)}, \tag{21}$$

$$\delta\kappa_t = \frac{q_+}{2\sinh(q_+ a)} - \frac{q_-}{2\sinh(q_- a)}, \tag{22}$$

and

$$\kappa = \frac{q_+}{2\tanh(q_+ a)} + \frac{q_-}{2\tanh(q_- a)}, \tag{23}$$

$$\delta\kappa = \frac{q_+}{2\tanh(q_+ a)} - \frac{q_-}{2\tanh(q_- a)}, \tag{24}$$

with $q_\pm^{-1}$ being the penetration length of a particle with a positive/negative chirality inside the barrier, and a is the barrier width. As the width of the barrier grows, the "tunneling" boundary coefficients decay exponentially, $\lim_{a\to\infty}\kappa_t = 0$. As expected, we see then that the coupling between the superconductor and the ferromagnet disappears, as does the proximity effect. Furthermore, if we "turn off" the spin-orbit coupling in the barrier (i.e., setting $\alpha_R = 0$, so that $q_+ = q_-$), we see that the spin-mixing terms vanish, $\delta\kappa = \delta\kappa_t = 0$, and we recover the standard boundary conditions for the proximity effect.

As in Eq. (11), we introduce a four-component state vector in the combined spin-Nambu space to describe the superconductor. The Pauli matrices in Nambu space will be denoted by $\hat{\tau}_x$, $\hat{\tau}_y$, and $\hat{\tau}_z$, and the unit matrix by $\hat{\tau}_0$. 4×4 matrices in the spin-Nambu space will be denoted by an inverse hat, for instance,

$$\check{T}_{\mathbf{p}} = \begin{pmatrix} \hat{T}_{\mathbf{p}} & 0 \\ 0 & \hat{T}^*_{-\mathbf{p}} \end{pmatrix}, \qquad \check{R}_{\mathbf{p}} = \begin{pmatrix} \hat{R}_{\mathbf{p}} & 0 \\ 0 & \hat{R}^*_{-\mathbf{p}} \end{pmatrix}, \tag{25}$$

where the asterisk denotes complex conjugation. Note that $\gamma_{-\mathbf{p}} = \gamma_{\mathbf{p}} + \pi$, therefore $\exp(i\gamma_{-\mathbf{p}}) = -\exp(i\gamma_{\mathbf{p}})$, as it appears in $\hat{T}^*_{-\mathbf{p}}$ and $\hat{R}^*_{-\mathbf{p}}$.

Using these notations, we can write the boundary conditions for the superconductor in the following form: $\frac{m_B}{m_S}\partial_z \overrightarrow{\Psi}^{(S)}_{\mathbf{p}}(-a) = \check{T}_{\mathbf{p}} \overrightarrow{\Psi}^{(F)}_{\mathbf{p}}(0) - \check{R}_{\mathbf{p}} \overrightarrow{\Psi}^{(S)}_{\mathbf{p}}(-a)$. We proceed by first incorporating the right side of this boundary condition into the Bogoliubov–de Gennes equation for a superconductor, which we symbolically write in the form[72]

$$\check{\breve{G}}^{-1}_{\mathbf{p}} \overrightarrow{\Psi}^{(S)}_{\mathbf{p}}(z) = -\frac{\hbar^2}{2m_B}\delta(z+a)\big[\check{T}_{\mathbf{p}} \overrightarrow{\Psi}^{(F)}_{\mathbf{p}}(0) - \check{R}_{\mathbf{p}} \overrightarrow{\Psi}^{(S)}_{\mathbf{p}}(-a)\big]. \tag{26}$$

Here, $\check{\breve{G}}_{\mathbf{p}}(z,z')$ is the Green function of the Bogoliubov–de Gennes equation for a bulk superconductor in the half-space, $z < -a$, which satisfies the von Neumann boundary conditions, $\partial_z \check{\breve{G}}_{\mathbf{p}}(z,z')|_{z=-a} = 0$. It can be expressed in terms of the Green function of an infinite bulk s-wave superconductor by the method of mirror images, and it reads

$$\check{\breve{G}}_{\mathbf{p}}(z,z') = \check{G}_{\mathbf{p}}(z-z') + \check{G}_{\mathbf{p}}(z+z'+2a), \tag{27}$$

where

$$\check{G}_{\mathbf{p}} = \begin{pmatrix} \hat{G}_{\mathbf{p}} & \hat{F}^*_{-\mathbf{p}} \\ \hat{F}_{\mathbf{p}} & \hat{G}^*_{-\mathbf{p}} \end{pmatrix} \tag{28}$$

and $\hat{G}_{\mathbf{p}}$ and $\hat{F}_{\mathbf{p}}$ are the normal and Gor'kov Green functions, respectively. Consequently, the solution to the Bogoliubov–de Gennes equation (26) is derived by convoluting the Green function with the boundary term on the right side of Eq. (26), which is simple due to the δ function in the latter,

$$\overrightarrow{\Psi}^{(S)}_{\mathbf{p}}(z) = -\frac{\hbar^2}{m_B}\check{G}_{\mathbf{p}}(z+a)\big[\check{T}_{\mathbf{p}} \overrightarrow{\Psi}^{(F)}_{\mathbf{p}}(0) - \check{R}_{\mathbf{p}} \overrightarrow{\Psi}^{(S)}_{\mathbf{p}}(-a)\big]. \tag{29}$$

For the purpose of understanding induced superconductivity in the ferromagnet, we only need to know the boundary value of the superconducting wave function at $z = -a$. From Eq. (29), we obtain

$$\overrightarrow{\Psi}^{(S)}_{\mathbf{p}}(-a) = -\frac{\hbar^2}{m_B}\frac{1}{1-(\hbar^2/m_B)\check{g}_{\mathbf{p}}\check{R}_{\mathbf{p}}}\check{g}_{\mathbf{p}}\check{T}_{\mathbf{p}} \overrightarrow{\Psi}^{(F)}_{\mathbf{p}}(0), \tag{30}$$

where

$$\check{g}_{\mathbf{p}} = \lim_{z\to -a} \check{G}_{\mathbf{p}}(z+a) = \int \frac{dp_z}{2\pi}\check{G}(p_x,p_y,p_z). \tag{31}$$

We note here that (30) is *exact* and that we have not used any properties of the system at $z > 0$ up to this point. Therefore, the equation above is applicable to any such junction with any normal or superconducting material at $z > 0$ (the only constraint is the continuity of derivatives at the $z = 0$ boundary, which may be violated if there is a spin Hall effect present. In this case, however, an alternative set of boundary conditions can be derived.)

3. Ferromagnet

The expression in Eq. (30), which represents a useful technical result of the paper, allows one to formulate a closed problem on the (ferromagnetic) normal side. Let us write the Schrödinger equation (4) as

$$\big[\check{G}^{(F)}_{\mathbf{p}}\big]^{-1} \circ \overrightarrow{\Psi}^{(F)}_{\mathbf{p}}(z) = 0, \tag{32}$$

where we have extended the equation into the Nambu space. The propagator $\check{G}^{(F)}_{\mathbf{p}}(z,z')$ describes a particle of the magnetized Fermi liquid in the shell $0 \leqslant z \leqslant d$. Apart from the trivial boundary condition (7) at the hard wall, (9) together with the solution of Sec. IV B 1 and (30) give rise to the following constraint:

$$\frac{m_B}{m_F}\partial_z \overrightarrow{\Psi}^{(F)}_{\mathbf{p}}(0) = \left[\check{R}_{\mathbf{p}} + \check{T}_{\mathbf{p}}\frac{\hbar^2/m_B}{1-\frac{\hbar^2}{m_B}\check{g}_{\mathbf{p}}\check{R}_{\mathbf{p}}}\check{g}_{\mathbf{p}}\check{T}_{\mathbf{p}}\right]\overrightarrow{\Psi}^{(F)}_{\mathbf{p}}(0). \tag{33}$$

The boundary condition (10) together with (32) and (33) form a self-consistent set for $z > 0$.

We assume at this point that the spin-orbit coupling energy scale is small compared to other relevant energies in the problem, and we keep the spin-orbit parameter α_R finite only where we otherwise would get a vanishing effect, i.e., in the spin-mixing terms. In all other quantities, we set $\alpha_R = 0$. This brings the reflection matrix to a simpler form proportional to the unit matrix,

$$\check{R}_{\mathbf{p}} \approx \kappa\check{1} \equiv \kappa\hat{\tau}_0\hat{\sigma}_0, \tag{34}$$

where κ is defined in Eq. (23). In the $\alpha_R \to 0$ limit, we have $\kappa = q/\tanh(qa)$, where $q = \sqrt{\frac{2m}{\hbar^2}(U_0 + \frac{\mathbf{p}^2}{2m_B} - \varepsilon)}$. In the limit of a high barrier, $\kappa \approx q$.

We now consider the operator denominator in the boundary condition (33). If the bulk superconductor is deep in the paired state, we may neglect the normal Green function and estimate the integrated Green function in Eq. (31) as $\check{g} \approx f\hat{\tau}_x(i\hat{\sigma}_y)$, with

$$f = \frac{1}{\hbar v_S}\frac{\Delta}{\sqrt{\Delta^2+\xi^2_{\mathbf{p}}}}. \tag{35}$$

Here, we have also ignored retardation effects. For small $\xi_{\mathbf{p}} = p^2/(2m_S) - \mu_S$, it can be estimated as $f \approx 1/(\hbar v_S)$, where v_S is the Fermi velocity in the superconductor. Therefore, the term in question from Eq. (33) becomes

$$\frac{\hbar^2}{m_B}\frac{1}{1-\frac{\hbar^2}{m_B}\check{g}_{\mathbf{p}}\check{R}_{\mathbf{p}}}\check{g}_{\mathbf{p}} \approx \frac{1}{\kappa}\frac{\alpha}{1+\alpha^2}[\hat{\tau}_x(i\hat{\sigma}_y) - \alpha\check{1}], \tag{36}$$

where $\alpha = \kappa f/m_B$. This parameter can be estimated as $\alpha \sim \sqrt{m_S U_0/m_B E^{(S)}_F}$. Note that the last term in Eq. (36) is uninteresting because it does not include any off-diagonal contributions in Nambu space. The term slightly renormalizes the boundary conditions for the transverse wave function in the ferromagnet. It can therefore be safely dropped.

Incorporating the right side of the boundary condition (33) into the Schrödinger equation for the ferromagnet (32), we obtain

$$\check{G}^{(F)-1}_{\mathbf{p}} \circ \overrightarrow{\Psi}^{(F)}_{\mathbf{p}}(z) = \frac{-\hbar^2\alpha\delta(z)}{2f\kappa m_B(1+\alpha^2)}\check{T}_{\mathbf{p}}\check{g}_{\mathbf{p}}\check{T}_{\mathbf{p}}\overrightarrow{\Psi}^{(F)}_{\mathbf{p}}(0). \tag{37}$$

This is the Bogoliubov–de Gennes equation for the normal region with superconducting correlations introduced via the

boundary term that carries information about all Andreev processes.

C. Proximity-induced superconducting gap

To calculate the superconducting gap induced in the ferromagnet, we assume that its magnetization is unaffected by the proximity to the superconductor, and we fix it instead of calculating it self-consistently. This should be valid in the low barrier transparency limit which we are considering here. We also focus on a particular subband with a given spin polarization and ignore intraband scattering (which is justified only in the clean case). Furthermore, we assume that the ferromagnetic layer or wire is very thin in the z direction, and we approximate the full solution as

$$\psi^{(F)}_{\alpha,\mathbf{p}}(z) = \chi_\alpha(\mathbf{m})\psi^{(\mathrm{tr})}(z)\phi(\mathbf{p}), \tag{38}$$

where $\chi_\alpha(\mathbf{m})$ is a spinor describing the magnetization direction that we wish to enforce and $\psi^{(\mathrm{tr})}(z)$ is the transverse envelope wave function that we approximate as a solution of the free one-dimensional Schödinger equation,

$$\left(\partial_z^2 + \frac{2m_F\varepsilon_{\mathrm{tr}}}{\hbar^2}\right)\psi^{(\mathrm{tr})}(z) = 0, \tag{39}$$

with the unusual boundary conditions valid for low barrier transparency,

$$\frac{m_B}{m_F}\partial_z\psi^{(\mathrm{tr})}(0) = \kappa\psi^{(\mathrm{tr})}(0), \qquad \psi^{(\mathrm{tr})}(d) = 0. \tag{40}$$

We then introduce solution (38) into (37), multiply it by $\psi^{(\mathrm{tr})*}(z)$, average it over the transverse direction, and extract the relevant spin component (a word of caution here is that the standard convention for the Gor'kov Green function taken proportional to $i\hat{\sigma}_y$ is basis-dependent and assumes spin quantization along the z axis).

For the ferromagnetic state polarized along z, we obtain the Bogoliubov–de Gennes equations in the familiar form

$$\left[\frac{\mathbf{p}^2}{2m_F} - (\mu_F - \varepsilon_{\mathrm{tr}})\right]\phi_{\mathbf{p}} + E_g(p_y + ip_x)\phi^*_{-\mathbf{p}} = 0, \tag{41}$$

where the proximity-induced gap or so-called minigap is

$$E_g = \frac{2f\hbar^4}{pm_B^2}\kappa_t\delta\kappa_t|\psi^{(\mathrm{tr})}(0)|^2. \tag{42}$$

The boundary value of the transverse wave function can be obtained from Eq. (39) and reads

$$|\psi^{(\mathrm{tr})}(0)|^2 = \frac{2}{d}\frac{1}{1+\xi^2+\xi/(k_{\mathrm{tr}}d)}, \tag{43}$$

where $\xi = m_F q/(m_B k_{\mathrm{tr}})$ and k_{tr} is a solution to the eigenvalue problem, $\tan(k_{\mathrm{tr}}d)/(k_{\mathrm{tr}}d) = -m_B/(m_F q d)$, which determines the spectrum, $\varepsilon_{\mathrm{tr}} = \hbar^2 k_{\mathrm{tr}}^2/(2m_B)$. We see from Eq. (42) that the proximity-induced minigap is extremely sensitive to the actual width of the normal region: the smaller the width, the more frequent the Andreev scattering processes, and the larger the minigap.[72]

V. MICROSCOPIC THEORY FOR THE RESISTANCE PEAK

In the preceding section, we considered the Andreev physics which takes place at a W-Co interface with Rashba spin-orbit coupling. We showed that the triplet p-wave proximity effect is suppressed due to the weak interface spin-orbit coupling, which facilitates the singlet-triplet conversion across the interface. With this result, we now formulate a theory for the observed resistance peak based on the physics of superconducting fluctuations in the W electrodes.

A. Effective dimensionality of a tungsten electrode for fluctuation analysis

Superconducting fluctuation physics depends critically on the dimensionality of the system, with the general trend being that the lower the dimensionality, the more pronounced and singular the fluctuation effects are. However, one should exercise care in determining the effective dimensionality of a system, as this notion depends on a particular effect that is being studied. For example, the system may be three-dimensional in terms of single-electron diffusion physics, but fall into the category of one-dimensional superconductors when it comes to the fluctuation analysis. We believe that such is the case with the W electrodes that host superconductivity and most of the fluctuation physics in the experiment under study involving $L_\perp^{(1)} \sim 250$ nm wide and $L_\perp^{(2)} \sim 100$ nm thick W strips.

The finiteness of the transverse directions implies that whenever we have an integral over a three-dimensional momentum, its transverse part must be replaced with a sum over quantized modes,

$$\int \frac{dq_\perp}{2\pi\hbar} f(q_\perp) \longrightarrow \frac{1}{L_\perp}\sum_{n_\perp} f\left(\frac{2\pi\hbar n_\perp}{L_\perp}\right).$$

For superconducting fluctuation analysis, the relevant function of interest is the fluctuation propagator, which appears in the combination

$$\frac{1}{L_\perp}\sum_{n_\perp}\left[D\left(\frac{2\pi\hbar n_\perp}{L_\perp}\right)^2 + Dq_{||}^2 + \tau_{\mathrm{GL}}^{-1}\right]^{-1}, \tag{44}$$

where $D = v_{\mathrm{F}}^2\tau/3$ is the diffusion coefficient, and the Ginzburg-Landau relaxation time,

$$\tau_{\mathrm{GL}} = \frac{\pi}{8}\frac{\hbar}{T - T_{\mathrm{c}}}, \tag{45}$$

tunes the proximity to the transition temperature T_{c}. Hereafter, we will focus on a superconducting electrode and assume that we are dealing there with a disordered superconductor.

The question of whether or not a particular dimension is important reduces to the comparison of the first and last term in the square brackets in Eq. (44). If the former is much larger than the latter for any $n_\perp \neq 0$ the corresponding dimension is unimportant and an effective reduction of dimensionality occurs. One can define the following characteristic temperature scale (to be compared with $T - T_{\mathrm{c}}$) as follows:

$$T_\perp(L_\perp) = \frac{1}{k_{\mathrm{B}}}\left(\frac{\pi^3}{6}\right)\left(\frac{l}{L_\perp}\right)\left(\frac{\hbar v_{\mathrm{F}}}{L_\perp}\right), \tag{46}$$

where v_{F} is the Fermi velocity, $l = v_{\mathrm{F}}\tau$ is the electron mean-free path, and we have restored the Boltzmann constant k_{B} and the Planck constant $\hbar$.

For W, the Fermi velocity can be estimated as $v_F \sim 0.5 \times 10^6$ m/s, and taking the largest of the two transverse dimensions $L_\perp \sim 250$ nm, we find

$$T_\perp^{\mathrm{W}}(250\ \mathrm{nm}) \sim \left(\frac{l}{L_\perp}\right) 80\ \mathrm{K}.$$

If we assume that the mean-free path in the amorphous W strips is of the order of a nanometer, the corresponding temperature scale becomes of order $T_\perp^{\mathrm{W}}(250\ \mathrm{nm}) \sim 0.3$–$1$ K, which is very reasonable and implies that as soon as we approach the superconducting transition with $(T - T_c) \ll T_c \sim 4.4$–$5$ K, we may view the electrode as a one-dimensional superconductor.

B. Fluctuation correction to the density of states

We now analyze the DOS fluctuation physics on the basis of the standard diagrammatic perturbation theory. The Cooper-channel correction to the electronic DOS is given by

$$\delta\nu(\epsilon) = -\frac{1}{\pi}\int \frac{d^d p}{(2\pi)^d}\mathrm{Im}\left\{\mathcal{G}^2(i\varepsilon_m,\mathbf{p})\Sigma(i\varepsilon_m,\mathbf{p})\right\}_{i\varepsilon_m\to\epsilon}, \quad (47)$$

where $\Sigma(i\varepsilon_m,\mathbf{p})$ is the self-energy described by the diagram in Fig. 4(a). It reads

$$\Sigma(i\varepsilon_m,\mathbf{p}) = -T\sum_{\Omega_n}\int \frac{d^d q}{(2\pi)^d}\mathcal{G}(i\Omega_n - i\varepsilon_m,\mathbf{q}-\mathbf{p}) \times \mathcal{C}^2(\varepsilon_m,\Omega_n-\varepsilon_m;\mathbf{q})\mathcal{L}(\Omega_n,\mathbf{q}), \quad (48)$$

where

$$\mathcal{G}(i\varepsilon_m,\mathbf{p}) = \frac{1}{i\tilde{\varepsilon}_m - \xi_{\mathbf{p}}} \quad (49)$$

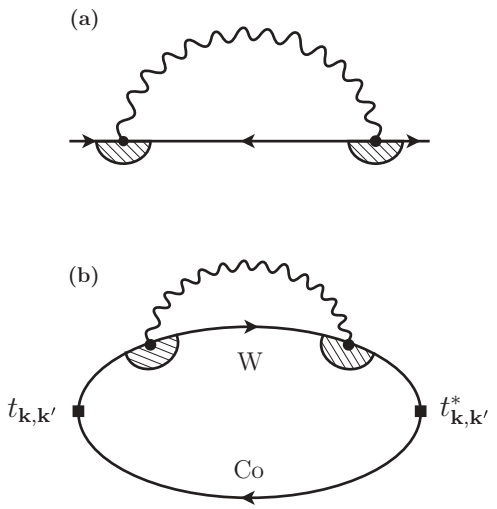

FIG. 4. (a) Self-energy diagram describing a correction to the single-electron Green function. The wavy line corresponds to the superconducting fluctuation propagator, and the shaded vertices represent Cooperon vertices. (b) A diagram corresponding to the lowest-order correction to the transport kernel due to superconducting fluctuations in the tungsten electrode. As labeled in the figure, the top (bottom) solid line represents the electron propagator for tungsten (cobalt).

is the Matsubara Green function with $\xi_{\mathbf{p}} = v_F(p - p_F)$ and $\tilde{\varepsilon}_m = \varepsilon_m + \mathrm{sgn}\,(\varepsilon_m)/(2\tau)$, τ is the scattering time,

$$\mathcal{C}(\varepsilon_m,\Omega_n-\varepsilon_m;\mathbf{q}) = \frac{1}{\tau}\frac{\theta[\varepsilon_m(\varepsilon_m-\Omega_n)]}{Dq^2+\gamma_s+|2\varepsilon_m-\Omega_n|} \quad (50)$$

is the Cooperon vertex, where we included the pair-breaking scattering rate $\gamma_s = 2/\tau_s$, and $\theta(\cdot)$ is the standard Heaviside step function. In the vicinity of the transition point, the fluctuation propagator reads

$$\mathcal{L}(\Omega_n,\mathbf{q}) = \frac{8T_c}{\pi\nu_0}\left[Dq^2 + \tau_{\mathrm{GL}}^{-1} + |\Omega_n|\right]^{-1}, \quad (51)$$

where $\tau_{\mathrm{GL}} = \frac{\pi}{8}\frac{\hbar}{T-T_c}$ and $\nu_0 = mp_F/2\pi^2$ is the bare DOS for a single spin projection. As per the usual convention, $\Omega_n = 2\pi nT$ denotes the bosonic Matsubara frequency and $\varepsilon_m = (2m+1)\pi T$ is the fermionic Matsubara frequency. Finally, note that the physical quantity of interest, the DOS, must be analytically continued from the discrete set of Matsubara frequencies to the continuum of real energies, as labeled by the symbol $i\varepsilon_m \to \epsilon$ in Eq. (47).

Since the tungsten electrodes are amorphous, we can safely assume that they are strongly disordered s-wave superconductors, where $T_c\tau \ll 1$ (but of course we also assume that we are far from localization, that is, $E_F\tau \gg 1$). In this case, the three-Green-function block takes the especially simple form

$$\nu_0\int d\xi\ \mathcal{G}(i\Omega_n - i\varepsilon_m,\mathbf{q}-\mathbf{p})\mathcal{G}^2(i\varepsilon_m,\mathbf{p}) = -2\pi i\nu_0\tau^2\mathrm{sgn}\,(\varepsilon_m), \quad (52)$$

where we enforced the constraint $\varepsilon_m(\varepsilon_m - \Omega_n) > 0$ in Eq. (50). This leads to the following expression for the DOS:

$$\delta\nu(\epsilon) = \frac{4}{\pi^3}\int\frac{d^d q}{(2\pi)^d}\left(\frac{\partial}{\partial\gamma_s}\right)\mathrm{Re}\,S^R(\mathbf{q},\epsilon), \quad (53)$$

where $S^R(\mathbf{q},\epsilon) = S(\mathbf{q},i\varepsilon_m\to\varepsilon)$ represents the analytically continued (retarded) Matsubara sum

$$S(\mathbf{q},\varepsilon_m>0) = \sum_{n=-\infty}^{m}\frac{1}{\left(\frac{Dq^2+\tau_{\mathrm{GL}}^{-1}}{2\pi T_c}+|n|\right)\left(\frac{Dq^2+\gamma_s}{2\pi T_c}+|2m+1-n|\right)}. \quad (54)$$

This sum can be calculated exactly in terms of the digamma function,

$$\psi(z) = -\gamma + \sum_{n=0}^{\infty}[(n+1)^{-1} - (n+z)^{-1}], \quad (55)$$

which is analytic everywhere except $z = 0, -1, -2, \ldots$. It is convenient to separate the sum (54) into two pieces, $\sum_{n=-\infty}^{0}\ldots$ and $\sum_{n=0}^{m}\ldots$. For the first term, the analytic continuation reduces to replacing $\varepsilon_m \to -i\varepsilon$. For the second term, it becomes possible after noticing the "reflection property," where $m-n$ can be replaced by $n-m$. This leaves the sum from $n=0$ to $n=m$ unchanged but the denominator "positively defined" and ready for analytic continuation. Finally, the asymptotic form of DOS in the limit of $\{\epsilon,\tau_{\mathrm{GL}}^{-1},\gamma_s\} \ll T \sim T_c$ becomes

$$S^R(\mathbf{q},\epsilon) = \frac{(2\pi T_c)^2}{\left(Dq^2+\tau_{\mathrm{GL}}^{-1}\right)\left(2Dq^2+\gamma_s+\tau_{\mathrm{GL}}^{-1}-2i\epsilon\right)}. \quad (56)$$

Let us now focus specifically on the correction to the DOS of electronic states with spin-up at the Fermi level, i.e., $\epsilon = 0$. The remaining elementary integrals in Eq. (53) can now be easily calculated, and we find

$$\delta\nu_\uparrow(0,T) = -\frac{\nu_0}{p_F^2 A}\frac{\sqrt{6\pi^7}}{128}\frac{T_c^2\tau^{-1/2}}{(T-T_c)^{5/2}}\frac{1+2\alpha(T)}{\alpha^3(T)[1+\alpha(T)]^2}, \tag{57}$$

where

$$\alpha(T) = \sqrt{\frac{1}{2}\left[1+\frac{\pi}{4}\frac{1}{(T-T_c)\tau_s}\right]}. \tag{58}$$

Here, A is the effective area of the fluctuating superconductor in the region where the fluctuations are studied (we expect it to be related to the dimensions of the superconductor-nanowire contact and, consequently, we expect A to be smaller than the cross-sectional area of the wire). Notice that in the absence of pair breaking and/or far from the transition, where $(T-T_c)\tau_s \gg 1$, (58) reduces to a constant $\alpha = 1/\sqrt{2}$ and the DOS at the Fermi level acquires a very sharp temperature dependence as follows:

$$\delta\nu_\uparrow(0,T) \propto -(T-T_c)^{-5/2} \quad \text{if} \quad (T-T_c)\tau_s \gg 1. \tag{59}$$

In the opposite regime of strong pair-breaking scattering or in the immediate vicinity of the transition, we find

$$\delta\nu_\uparrow(0,T) \propto -(T-T_c)^{-1/2} \quad \text{if} \quad (T-T_c)\tau_s \ll 1. \tag{60}$$

C. Fluctuation correction to the contact resistance

The result for the DOS at the Fermi level provides a useful insight into the physics near the transition and illustrates that, as a precursor to the global pairing transition, electrons are actively swept from the vicinity of the Fermi level due to the formation of the fluctuating Cooper pairs. However, the stand-alone quantity $\delta\nu(0,T)$ is not extremely useful for comparison with experiment, as it is actually not directly measurable. What is measured in experiment is resistance, which is an integral quantity that includes excitations with different energies and that has contributions from both single-electron transport across the W-Co junction and pair transport. As found in Sec. IV, the latter is suppressed strongly far from the transition due to the very small pair tunneling probability, which requires spin-orbit-assisted spin flips. Single-electron transport, on the other hand, does not rely on any spin-orbit coupling, and spin-up electrons can tunnel freely from the electrodes into the ferromagnet. Hence, there is a regime close to the transition (but still far enough from the immediate vicinity where the Cooper pairs eventually take over) where the single-electron tunneling dominates and is already strongly suppressed by fluctuations. This results in the upturn in the resistance as $T \to T_c^+$.

If we now focus entirely on single-electron transport and disregard pair-breaking scattering, we would tend to conclude (incorrectly) that the tunneling resistance acquires a contribution proportional to that in Eq. (59). This, however, is not so and the correction to the conductance is much weaker. This is because the tunneling electrons involve not only those precisely at the Fermi level, but all electron excitations within the shell of energies $E \sim (E_F - T, E_F + T)$. Hence, what matters is a redistribution of the DOS beyond the shell of energies that participate in transport (any redistribution within the shell is essentially not observable).

All these phenomena are automatically accounted for within the standard diagrammatic theory of transport. Here, we proceed nearly in a one-to-one correspondence with Ref. 75. The tunneling current is derived from the transport kernel $Q(\omega_l)$ shown in Fig. 4(b),

$$I(V) = -e\,\mathrm{Im}\,Q^R(\omega)|_{\omega=eV}, \tag{61}$$

where $Q^R(\omega)$ is the analytically continued transport kernel and V is the voltage across the tunneling contact. In the setup under consideration, the Matsubara transport kernel reads explicitly

$$\begin{aligned} Q(\omega_l) = -T^2 \sum_{\varepsilon_m;\Omega_n;\mathbf{k},\mathbf{k}'} |t_{\mathbf{k},\mathbf{k}'}|^2 \mathcal{G}_W^2(\varepsilon_m,\mathbf{k})\mathcal{G}_{Co}(\varepsilon_m+\omega_l,\mathbf{k}') \\ \times \int \frac{dq}{2\pi A}\mathcal{L}(\Omega_n,\mathbf{q})\mathcal{C}^2(\varepsilon_m,\Omega_n-\varepsilon_m;\mathbf{q}) \\ \times \mathcal{G}_W(\Omega_n-\varepsilon_m,\mathbf{q}-\mathbf{k}), \end{aligned} \tag{62}$$

where $t_{\mathbf{k},\mathbf{k}'}$ is the tunneling amplitude between two momentum states, $\mathcal{G}_{W/Co}(\varepsilon_m,\mathbf{k})$ is the electron Green function for the W electrode/Co nanowire, and all other quantities have been defined in Sec. V B. Following Ref. 75, we introduce a normal state resistance of the W-Co x junction $R^{(0)}_{W/Co}$ and obtain

$$\begin{aligned} Q(\omega_l) = \frac{\pi T^2}{2e^2 R^{(0)}_{W/Co}} \sum_{\varepsilon_m,\Omega_n} \mathrm{sgn}(\varepsilon_m)\,\mathrm{sgn}(\varepsilon_m+\omega_l) \\ \times\theta[\varepsilon_m(\varepsilon_m-\Omega_n)] \int \frac{dq}{2\pi A}\frac{\mathcal{L}(\Omega_n,\mathbf{q})}{(Dq^2+|2\varepsilon_m-\Omega_n|)^2}. \end{aligned} \tag{63}$$

Repeating the dimensionality-independent summations as in Ref. 75 [note that the clean case[75] becomes technically equivalent to the dirty case if we notice that the frequency dependence of the three-Green-function block in the reference is identical to that in the two Cooperons that appear in Eq. (2)] and evaluating the remaining integral over momentum q, we obtain the nonlinear I-V dependence,

$$\begin{aligned} I(V) = -\frac{T}{8\pi^2 e}\sqrt{\frac{3\pi}{2}}\frac{1}{R^{(0)}_{W/Co}\nu_0 v_F A}\mathrm{Im}\,\psi'\left[\frac{1}{2}-\frac{ieV}{2\pi T}\right] \\ \times \frac{1}{\sqrt{(T-T_c)\tau}}, \end{aligned} \tag{64}$$

where $\psi(\cdot)$ is the logarithmic derivative of the gamma function. The fluctuations correction to the differential conductance, dI/dV, is plotted in Fig. 5. Now focusing on the linear response regime, $\frac{dI}{dV}|_{V=0}$, we find the leading fluctuation correction to the W-Co contact resistance as follows:

$$\frac{\delta R^{(DOS)}_{W/Co}}{R^{(0)}_{W/Co}} = \frac{7\zeta(3)}{4\pi}\sqrt{\frac{3\pi}{2}}\frac{1}{p_F^2 A}\frac{1}{\sqrt{(T-T_c)\tau}}, \tag{65}$$

where $\zeta(z)$ is the Riemann zeta function and $\zeta(3) \approx 1.202$. The result in Eq. (65) corresponds to a sharp upturn in the resistance upon approaching the superconducting transition of the electrode.

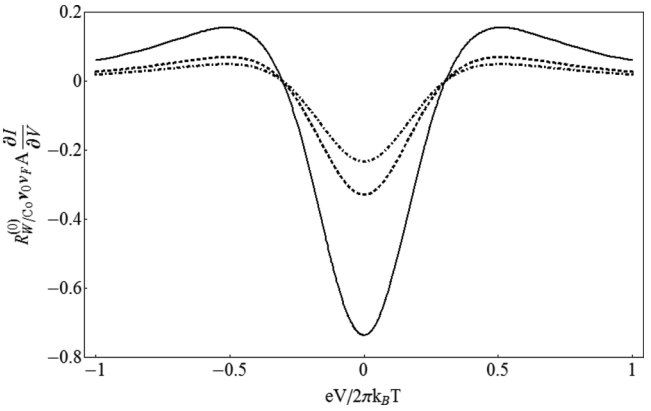

FIG. 5. Correction to the differential conductance from superconducting fluctuations as a function of dimensionless voltage $eV/2\pi T$ [see Eq. (64)]. The three curves correspond to different temperatures: $t := (T - T_c)\tau = 0.01$ for the solid line, $t = 0.05$ for the dashed line, and $t = 0.1$ for the dotted line.

D. Estimate of tunneling resistance due to fluctuating pairs

As emphasized throughout this section, the fluctuating Cooper pairs that appear in the electrodes do not aid with transport through the ferromagnetic nanowire initially because of their poor ability to tunnel into it. However, the experimental fact that the wire that is as long as a micrometer does become superconducting ensures that the pairs eventually are able to tunnel. Section IV provides a microscopic picture of the Andreev reflection/boundary physics that presumably makes this possible. Therefore, we expect that as the temperature is tuned down to the closest vicinity of the transition, the Cooper pair tunneling takes over the effect of the suppression of the DOS and the upturn in the resistance crosses over to the downturn going through a peak, as observed in experiment.

We notice here in passing that the height of the peak may provide a valuable insight into the competition of the two phenomena and may potentially become a means to measure the boundary spin-orbit coupling that is crucial for the proximity-induced p-wave superconductivity in the wire, which is a phenomenon of major interest. However, we leave the complicated microscopic theory of spin-orbit-assisted fluctuating pair tunneling for future studies, and in this section we only extract the leading temperature dependence of this AL type correction. It can be done on the basis of the Ambegaokar-Baratoff formula, which yields[52]

$$\delta R^{(\mathrm{AL})}_{\mathrm{W/Co}} \propto -\delta(\alpha_R) \int_{-\infty}^{\infty} d\varepsilon \frac{[\delta\nu(\varepsilon)]^2}{\cosh^2\left(\frac{\varepsilon}{2T}\right)}, \tag{66}$$

where $\delta\nu(\varepsilon)$ is the suppression of the DOS obtained in Sec. V B and we kept a small coefficient $\delta(\alpha_R)$ that includes spin-orbit suppression of the pair-tunneling as obtained in Sec. IV.

Note that the integral of the DOS over all energies vanishes identically, $\int_{-\infty}^{\infty} d\varepsilon\, \delta\nu(\varepsilon) = 0$ (the physical interpretation being that the total electron density is conserved and the electrons can only be redistributed across different energies), and a nonzero correction to the resistance in the first order appears only due to the modulating function, $\cosh^{-2}(\frac{\varepsilon}{2T})$, and consequently is much weaker [see Eq. (65)] than that in the DOS [see Eq. (59)]. For the pair tunneling, the situation is different as $\int_{-\infty}^{\infty} d\varepsilon\, \delta\nu^2(\varepsilon)$ is not only nonzero but is a very singular function near the transition. This singularity determines the scaling of the AL correction (66) as

$$\delta R^{(\mathrm{AL})}_{\mathrm{W/Co}} \propto -\frac{\delta(\alpha_R)}{(T - T_c)^4}. \tag{67}$$

VI. SUMMARY AND CONCLUSIONS

In this work, we study temperature-dependent transport through a ferromagnetic Co nanowire proximity-coupled to superconducting W electrodes. The work is motivated by a recent experiment,[21] in which the long-ranged superconducting proximity effect was observed in single-crystal Co nanowires coupled to conventional superconductors. The main focus of the work is on the large and sharp resistance peak which is observed at a temperature slightly above the transition temperature of the electrodes. We study in detail the resistance across a W-Co interface, which we argue is the dominant source of impedance in the transport. We first explore the possibility of inducing (even-frequency) p-wave pair correlations in an itinerant ferromagnet via Rashba spin-orbit coupling at the interface. We derive an expression for the induced p-wave minigap in terms of the microscopic parameters of the junction, and we argue that the pair transport across the interface is strongly suppressed due to the weak spin-orbit coupling. We then show how the anomalous resistance peak can be explained within the physics of superconducting fluctuations. In particular, we develop a microscopic theory for the superconducting fluctuation corrections in the W electrodes, and we show how these corrections can lead to an upturn in the resistance across the W-Co interface. While microscopic calculations are carried out for corrections to lowest order in tunneling, a more detailed microscopic calculation for (two-particle) pair transport is still needed to perform a quantitative fit to the resistance peak observed in experiment. In principle, a rigorous fit to the resistance peak may potentially be used to estimate the size of the interfacial spin-orbit coupling; this will be a topic of future work.[76]

It will be interesting to experimentally test the spin-orbit-assisted scenario by inserting a material with strong spin-orbit coupling (X) in between a superconductor and a ferromagnet by producing a junction of the type S/X/F/X/S.[77] Critical current as a function of the ferromagnet thickness has been studied for an S/F/S junction, but no evidence of spin-triplet correlations was observed.[78] The S/X/F/X/S junction may provide an alternative route to realizing spin-triplet correlations inside a ferromagnet besides the use of noncollinear ferromagnets.[22,23] We also note that the spin-orbit-assisted proximity-effect scenario considered here is different from the diffusive ferromagnet case, where the likely mechanism for the proximity effect is believed to be odd-frequency pairing.[23,24] The main argument for odd-frequency superconductivity is that any anisotropic pairing would decay fast into a disordered metal on a length scale of the order of a mean-free path, while odd-frequency isotropic pairing is immune from nonmagnetic static disorder. This result follows from the Usadel equation if we assume that the non-s-wave part of the disorder-averaged condensate wave function is small. Then upon linearization of

the Usadel equation, further exponential decay of the disorder-averaged p-wave condensate wave function inevitably follows. We note, however, that in certain geometries (e.g., if the mean-free path is much larger than the cross section of the wire, but much smaller than its length), there is no reason to assume that the anisotropic component is small locally near the contacts, and consequently the conventional derivation of the Usadel equations from the Eilenberger equations breaks down in these regions. With such an assumption about the boundary conditions, the correlator of p-wave condensate wave functions is not expected to decay exponentially at $T = 0$, in sharp contrast to the exponential decay of the disorder-averaged p-wave condensate wave function.[64,79,80] These mesoscopic fluctuation effects will be considered in detail elsewhere.[76]

A. Topological superconductivity and Majorana fermions

The canonical Kitaev model,[30] which is the simplest prototype of a one-dimensional topological superconductor, involves one fermion species hopping in a one-dimensional chain and subject to a prescribed p-wave pairing field on the nearest-neighbor bonds. The end points of the chain host single Majorana excitations that are of key interest. One can consider $\mathcal{N}$ replicas of the Kitaev-Majorana model with different p-wave pairing fields for each species but with no mixing between them, i.e., no interband pairing. If $\mathcal{N}$ is even, the end Majoranas are unstable against various perturbations and generally hybridize into relatively uninteresting finite-energy boundary states. In contrast, if $\mathcal{N}$ is odd, the system can then host one Majorana zero-energy state at each end. Indeed, recent theoretical works have addressed a multichannel generalization of Majorana end states in quasi-one-dimensional structures with Rashba spin-orbit coupling.[81–84] The works show that the Majorana end states are realized in some parameter regime as long as an odd number of transverse subbands are occupied and the width of the wire does not greatly exceed the superconducting coherence length.

The well-known difficulty in realizing the regime where (no. of end Majoranas) mod $2 = 1$ is of course related to the fact that the electrons have spin and consequently come in pairs. Therefore, according to Kitaev,[30] one necessarily, but not sufficiently, needs to break time-reversal symmetry in the one-dimensional superconductor to render it topological. The notable and fascinating proposals in which this regime was theoretically shown to be possible include a hybrid structure involving an s-wave superconductor/spin-orbit-coupled wire/ferromagnet,[35,44] a similar heterostructure without a ferromagnet but in a magnetic field,[36,42] a topological insulator/superconductor in a field,[31,45] and a half-metal/superconductor with spin-orbit coupling in the latter.[43]

If our interpretation of the experimental data in Ref. 21 is correct, we see that this work potentially possesses all the necessary ingredients for the realization of the Majorana end states, i.e., it has a ferromagnetic crystalline wire in which p-wave superconductivity has been induced. The $\mathcal{N}$-replica Kitaev-Majorana model discussed here should apply to a quasi-one-dimensional Co wire deposited on top of a three-dimensional W superconductor. In light of the multichannel generalization for the Majorana end states,[81–84] the Co nanowire does not necessarily have to be in a strictly one-dimensional limit. In fact, Ref. 84 showed that in the presence of disorder, an optimal nanowire system may require a few occupied subbands in order to create stable Majorana end states. Since Co is not a half-metal, the question is also whether a ferromagnetic wire, with both majority and minority carriers, can still host an odd number of end Majorana fermions. This should be possible in principle, because what we need is not necessarily to eliminate completely a spin component but merely to make the two components different from each other such that the total number of occupied subbands is odd, i.e., $(\mathcal{N}_\uparrow + \mathcal{N}_\downarrow) \bmod 2 = 1$. In the simplest model with no intersubband mixing, this would imply topological superconductivity. However, we mention that a single-species p-wave superconductor, more akin to the original proposal by Kitaev,[30] may be possible if the Co wire is replaced by a similar wire made of a half-metal such as CrO_2.

Reference 21 and the discussion above suggest an even simpler experimental setup for topological superconductivity. Indeed, realizing a one-dimensional topological superconductor using spinful fermions requires lifting the double degeneracy imposed by time-reversal symmetry. In principle, this can be achieved by proximity-inducing a Zeeman gap[35] or by applying an external magnetic field.[36,41] An alternative approach to realizing a one-dimensional topological superconductor is to deposit a ferromagnetic semiconductor wire on top of a ferromagnetic superconductor.[1–4] A particularly attractive candidate ferromagnetic semiconductor is europium oxide (EuO), which is known to possess nearly spin-polarized bands.[85,86] EuO becomes ferromagnetic below 70 K under ambient pressure, and the Curie temperature is known to increase with pressure, reaching 200 K under 1.5×10^5 atmospheres.[87] Ever since its integration with Si and GaN,[86] EuO has garnered much attention for its potential use in spintronic applications. Ferromagnetic superconductors are materials that exhibit an intrinsic coexistence of superconductivity and ferromagnetism where the same electrons are believed to be superconducting and ferromagnetic simultaneously. Perhaps the most well-known experimental realizations of ferromagnetic superconductors are uranium-based compounds. Following the first experimental realization a decade ago, there are now four such compounds,[1–4] two of which exhibit the phenomena at ambient pressures.[2,3] We propose that depositing URhGe electrodes on the EuO wire, in the arrangement shown in Fig. 1(a), would be conceptually the simplest structure to realize Majorana fermions that would require neither topological insulators nor control over spin-orbit couplings. Application of a magnetic field can further stabilize both the ferromagnetism and the superconducting phase.

ACKNOWLEDGMENTS

V.G. would like to thank K. Efetov, S. Das Sarma, Y. Oreg, J. Paglione, G. Tkachov, and A. Varlamov for discussions. S.T. would like to thank J. Wang for sharing experimental data, and J. R. Anderson, N. O. Birge, and M. Cuoco for discussions. S.T. would also like to thank J. D. Sau for stimulating discussions at an early stage of the work. S.T. was supported by DOE and V.G. was supported by DOE-BES (DESC0001911).

[1] S. S. Saxena *et al.*, Nature (London) **406**, 587 (2000).
[2] D. Aoki *et al.*, Nature (London) **413**, 613 (2001).
[3] N. T. Huy, A. Gasparini, D. E. de Nijs, Y. Huang, J. C. P. Klaasse, T. Gortenmulder, A. de Visser, A. Hamann, T. Görlach, and H. V. Löhneysen, Phys. Rev. Lett. **99**, 067006 (2007).
[4] T. Akazawa *et al.*, J. Phys.: Condens. Matter **16**, L29 (2004).
[5] C. Pfleiderer *et al.*, Nature (London) **412**, 58 (2001).
[6] L. Bauernfeind, W. Widder, and H. Braun, Physica C **254**, 151 (1995).
[7] C. Bernhard, J. L. Tallon, C. Niedermayer, T. Blasius, A. Golnik, E. Brucher, R. K. Kremer, D. R. Noakes, C. E. Stronach, and E. J. Ansaldo, Phys. Rev. B **59**, 14099 (1999).
[8] D. J. Pringle, J. L. Tallon, B. G. Walker, and H. J. Trodahl, Phys. Rev. B **59**, 11679 (1999).
[9] V. G. Hadjiev *et al.*, Phys. Status Solidi B **211**, R5 (1999).
[10] S. K. Sinha, G. W. Crabtree, D. G. Hinks, and H. Mook, Phys. Rev. Lett. **48**, 950 (1982).
[11] J. W. Lynn, G. Shirane, W. Thomlinson, R. N. Shelton, and D. E. Moncton, Phys. Rev. B **24**, 3817 (1981).
[12] J. W. Lynn, J. A. Gotaas, R. W. Erwin, R. A. Ferrell, J. K. Bhattacharjee, R. N. Shelton, and P. Klavins, Phys. Rev. Lett. **52**, 133 (1984).
[13] C.-K. Hsu *et al.*, J. Appl. Phys. **109**, 07B528 (2011).
[14] D. A. Dikin, M. Mehta, C. W. Bark, C. M. Folkman, C. B. Eom, and V. Chandrasekhar, Phys. Rev. Lett. **107**, 056802 (2011).
[15] J. A. Bert *et al.*, Nat. Phys. **7**, 767 (2011).
[16] A. I. Buzdin, Rev. Mod. Phys. **77**, 935 (2005).
[17] M. Giroud, H. Courtois, K. Hasselbach, D. Mailly, and B. Pannetier, Phys. Rev. B **58**, 11872(R) (1998).
[18] V. T. Petrashov, I. A. Sosnin, I. Cox, A. Parsons, and C. Troadec, Phys. Rev. Lett. **83**, 3281 (1999).
[19] V. Pena, Z. Sefrioui, D. Arias, C. Leon, J. Santamaria, M. Varela, S. J. Pennycook, and J. L. Martinez, Phys. Rev. B **69**, 224502 (2004).
[20] R. S. Keizer *et al.*, Nature (London) **439**, 825 (2006).
[21] J. Wang *et al.*, Nat. Phys. **6**, 389 (2010).
[22] T. S. Khaire, M. A. Khasawneh, W. P. Pratt, Jr., and N. O. Birge, Phys. Rev. Lett. **104**, 137002 (2010).
[23] F. S. Bergeret, A. F. Volkov, and K. B. Efetov, Phys. Rev. Lett. **86**, 4096 (2001).
[24] F. S. Bergeret, A. F. Volkov, and K. B. Efetov, Rev. Mod. Phys. **77**, 1321 (2005).
[25] V. L. Berezinskii, JETP Lett. **20**, 287 (1974).
[26] M. Eschrig, J. Kopu, J. C. Cuevas, and G. Schön, Phys. Rev. Lett. **90**, 137003 (2003).
[27] M. Eschrig and T. Löfwander, Nat. Phys. **4**, 138 (2008).
[28] F. Konschelle, J. Cayssol, and A. Buzdin, Phys. Rev. B **82**, 180509(R) (2010).
[29] L. Trifunovic and Z. Radović, Phys. Rev. B **82**, 020505(R) (2010).
[30] A. Yu. Kitaev, Phys. Usp. **44**, 131 (2001).
[31] L. Fu and C. L. Kane, Phys. Rev. Lett. **100**, 096407 (2008).
[32] Y. Tanaka, T. Yokoyama, and N. Nagaosa, Phys. Rev. Lett. **103**, 107002 (2009).
[33] M. Sato and S. Fujimoto, Phys. Rev. B **79**, 094504 (2009).
[34] M. Sato, Y. Takahashi, and S. Fujimoto, Phys. Rev. B **82**, 134521 (2010).
[35] J. D. Sau, R. M. Lutchyn, S. Tewari, and S. Das Sarma, Phys. Rev. Lett. **104**, 040502 (2010).
[36] R. M. Lutchyn, J. D. Sau, and S. Das Sarma, Phys. Rev. Lett. **105**, 077001 (2010).
[37] Y. Oreg, G. Refael, and F. von Oppen, Phys. Rev. Lett. **105**, 177002 (2010).
[38] V. Shivamoggi, G. Refael, and J. E. Moore, Phys. Rev. B **82**, 041405(R) (2010).
[39] P. A. Ioselevich and M. V. Feigel'man, Phys. Rev. Lett. **106**, 077003 (2011).
[40] S. B. Chung, H.-J. Zhang, X.-L. Qi, and S.-C. Zhang, Phys. Rev. B **84**, 060510 (2011).
[41] P. A. Lee, arXiv:0907.2681 (unpublished).
[42] J. Alicea, Phys. Rev. B **81**, 125318 (2010).
[43] M. Duckheim and P. W. Brouwer, Phys. Rev. B **83**, 054513 (2011).
[44] S. Tewari, J. D. Sau, and S. Das Sarma, Ann. Phys. (NY) **325**, 219 (2010).
[45] A. Cook and M. Franz, Phys. Rev. B **84**, 201105(R) (2011).
[46] P. Santhanam, C. C. Chi, S. J. Wind, M. J. Brady, and J. J. Bucchignano, Phys. Rev. Lett. **66**, 2254 (1991).
[47] M. Park, M. S. Isaacson, and J. M. Parpia, Phys. Rev. B **55**, 9067 (1997).
[48] K. Yu. Arutyunov, D. A. Presnov, S. V. Lotkhov, A. B. Pavolotski, and L. Rinderer, Phys. Rev. B **59**, 6487 (1999).
[49] P. Cadden-Zimansky, Z. Jiang, and V. Chandrasekhar, New J. Phys. **9**, 116 (2007).
[50] F. J. Jedema, B. J. van Wees, B. H. Hoving, A. T. Filip, and T. M. Klapwijk, Phys. Rev. B **60**, 16549 (1999).
[51] V. I. Fal'ko, A. F. Volkov, and C. Lambert, Phys. Rev. B **60**, 15394 (1999).
[52] A. I. Larkin and A. A. Varlamov, in *Superconductivity: Conventional and Unconventional Superconductors*, edited by K. H. Bennemann and J. B. Ketterson, Chap. 10 (Springer, Berlin, 2004), p. 369.
[53] A. A. Varlamov, G. Balestrino, E. Milani, and D. V. Livanov, Adv. Phys. **48**, 655 (1999).
[54] L. P. Gor'kov and E. I. Rashba, Phys. Rev. Lett. **87**, 037004 (2001).
[55] V. M. Edelstein, Phys. Rev. B **67**, 020505 (2003).
[56] J. R. Anderson and J. E. Schirber, J. Appl. Phys. **52**, 1630 (1981).
[57] F. Batallan, I. Rosenman, and C. B. Sommers, Phys. Rev. B **11**, 545 (1975).
[58] C. M. Singal and T. P. Das, Phys. Rev. B **16**, 5068 (1977).
[59] G. J. McMullan, D. D. Pilgram, and A. Marshall, Phys. Rev. B **46**, 3789 (1992).
[60] A. C. Potter and P. A. Lee, Phys. Rev. B **85**, 094516 (2012).
[61] S. LaShell, B. A. McDougall, and E. Jensen, Phys. Rev. Lett. **77**, 3419 (1996).
[62] C. R. Ast, D. Pacilé, L. Moreschini, M. C. Falub, M. Papagno, K. Kern, M. Grioni, J. Henk, A. Ernst, S. Ostanin, and P. Bruno, Phys. Rev. B **77**, 081407(R) (2008); C. R. Ast, J. Henk, A. Ernst, L. Moreschini, M. C. Falub, D. Pacil'e, P. Bruno, K. Kern, and M. Grioni, Phys. Rev. Lett. **98**, 186807 (2007).
[63] J. W. A. Robinson, S. Piano, G. Burnell, C. Bell, and M. G. Blamire, Phys. Rev. Lett. **97**, 177003 (2006).
[64] F. Zhou and B. Spivak, arXiv:cond-mat/9906177 (unpublished).
[65] L. B. Ioffe, A. I. Larkin, A. A. Varlamov, and L. Yu, Phys. Rev. B **47**, 8936 (1993).
[66] G. Balestrino, M. Marinelli, E. Milani, A. A. Varlamov, and L. Yu, Phys. Rev. B **47**, 6037 (1993).
[67] G. Balestrino, E. Milani, and A. A. Varlamov, Physica C **210**, 386 (1993).
[68] V. M. Galitski and A. I. Larkin, Phys. Rev. B **63**, 174506 (2001).

[69]I. S. Beloborodov, K. B. Efetov, A. V. Lopatin, and V. M. Vinokur, Rev. Mod. Phys. **79**, 469 (2007).
[70]We note that what we call the "Aslamazov-Larkin" contribution here is not strictly the same as the contribution of the same name considered for transport through bulk disordered superconductors. In this work, the transport is considered across a ferromagnet-superconductor interface. What we refer to as the Aslamazov-Larkin contribution is the transport of Cooper pairs across this interface.
[71]A. F. Volkov, P. H. C. Magnee, B. J. van Wees, and T. M. Klapwijk, Physica C **242**, 261 (1995).
[72]G. Tkachov, Physica C **417**, 127 (2005).
[73]R. Strack and D. Vollhardt, Phys. Rev. Lett. **72**, 3425 (1994).
[74]G. Annunziata, H. Enoksen, J. Linder, M. Cuoco, C. Noce, and A. Sudbo, Phys. Rev. B **83**, 144520 (2011).
[75]C. Di Castro, R. Raimondi, C. Castellani, and A. A. Varlamov, Phys. Rev. B **42**, 10211 (1990).
[76]S. Takei and V. Galitski (unpublished).
[77]N. Birge and M. Cuoco (private communication).
[78]M. A. Khasawneh, W. P. Pratt Jr., and N. O. Birge, Phys. Rev. B **80**, 020506(R) (2009).
[79]F. Zhou and B. Spivak, Phys. Rev. Lett. **80**, 5647 (1998).
[80]V. M. Galitski and A. I. Larkin, Phys. Rev. Lett. **87**, 087001 (2001).
[81]A. C. Potter and P. A. Lee, Phys. Rev. Lett. **105**, 227003 (2010).
[82]A. C. Potter and P. A. Lee, Phys. Rev. B **83**, 094525 (2011).
[83]R. M. Lutchyn, T. D. Stanescu, and S. Das Sarma, Phys. Rev. Lett. **106**, 127001 (2011).
[84]T. D. Stanescu, R. M. Lutchyn, and S. Das Sarma, Phys. Rev. B **84**, 144522 (2011).
[85]P. G. Steeneken, L. H. Tjeng, I. Elfimov, G. A. Sawatzky, G. Ghiringhelli, N. B. Brookes, and D.-J. Huang, Phys. Rev. Lett. **88**, 047201 (2002).
[86]A. Schmehl *et al*., Nat. Mater. **6**, 882 (2007).
[87]N. M. Souza-Neto, D. Haskel, Y.-C. Tseng, and G. Lapertot, Phys. Rev. Lett. **102**, 057206 (2009).